Linear conductances of gated graphene structures with selected connectivity

L. Ulčakar, †,‡ T. Rejec, †,‡ and A. Ramšak *,†,‡

J. Stefan Institute, Ljubljana, Slovenia, and Faculty of mathematics and physics,
University of Ljubljana, Ljubljana, Slovenia

E-mail: anton.ramsak@ijs.si

In the memory of Janez (Janko) Jamnik

 $_3$ Abstract

The ratio of conductances through carbon-ring based molecules are calculated for various positions of source-drain electrode leads on the molecule. These ratios are usually integers – the so-called magic numbers. We find that deviations of the magic number ratios are either zero or quadratic in ratios of tight-binding model parameters.

Introduction

1

2

- 9 Charge transport through nanostructures represents a challenge from the experimental point
- of view as well as for theoretical approaches¹. Most of experimental work so far has been
- done for semiconducting structures² as promising candidates for tailoring various electronic
- devices, such as single electron transistors³ and charge or spin quantum bits⁴. One of the
- advantages of semiconductor techology is its versitility in formating structures on demand,

^{*}To whom correspondence should be addressed

[†]J. Stefan Institute

[‡]University of Ljubljana

with reliable and reproducible gating and connectivity to external leads. A disadvantage of these structures is their relatively large spatial extend limiting functional operation to low temperatures. For possible applications to sensors or quantum infromation processing devices room-temperatures operation is desired, which demands reduction of device size leading to larger energy scale. Molecules connected to metalic leads therefore represent ideal candidates for devices where phase-coherent transport between attached electrondes is required at moderate temperatures ^{5,6}.

In general, nanostructures exhibit an extremely rich spectrum of quantum phenomena.

In particular, in conductance measurements strong electron-electron interaction leads to

Coulomb blockade⁷, the Kondo effect⁸, various spin dependent anomalies^{9,10} or instabili
ties due to vibrational degrees of freedom, where different electron-phonon interactions can

play an important role^{11,12}. Due to large coherence lengths in clean structures, interference

effects also play an essential role in transport through the nano-device, as was recently stud
ied experimentally even at room temperature^{13–21}. Small graphene based nanostructures

are well-defined since they are nearly defect-free which enables reproducible conductance

measurements exibiting subtle interference effects^{22–24}.

Here we concentrate on "magic" ratios, found recently in connectivity driven electrical 30 conductance of graphene-like aromatic molecules ²⁵. Theoretical analysi of experiments using 31 mechanically controlled break junctions to measure electrical conductance of such molecules 32 reveal specific ratios between different connectivity geometry of external leads. These magic 33 ratios appear in the regime of particle-hole symmetrically filled molecules, where the chemical potential is located at the HOMO-LUMO mid-gap. Numerical analysis has been performed 35 for a tight-binding approximation of a molecule weakly coupled to charge reservoirs connected to the graphene molecule via linear carbon chains referred to as source and drain leads. In this paper we analyse the stability of magic numbers, with respect to changes of the coupling to the leads and also due to changing to potential of top gates (not shown) which in turn 39 change the electron occupation of the molecule.

41 Model and methods

- We consider polycyclic aromatic hydrocarbon-like graphene structures, coupled to two met-
- alic electrodes, via source and drain leads. This is shown schematically in Fig. 1 for the case
- 44 of a benzene molecule.

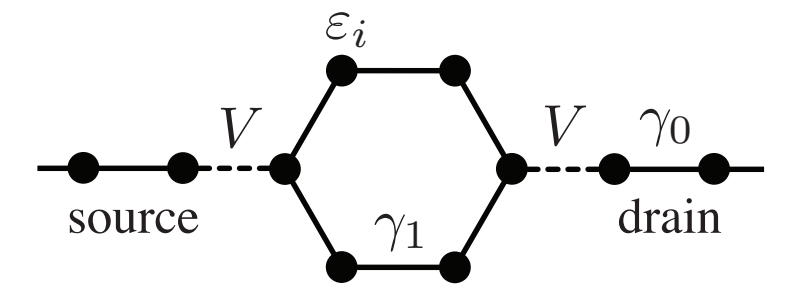


Figure 1: A benzene-like structure (molecule) attached to the leads.

To model such a system we adopt the effective Hamiltonian

$$H = H_{\text{molecule}} + H_{\text{leads}} + H_{\text{coupling}}$$

where the molecule is described in terms of a tight-binding Hamiltonian

$$H_{\text{molecule}} = \sum_{i,\sigma} \varepsilon_i n_{i,\sigma} - \sum_{i,j,\sigma} \gamma_{ji} c_{j,\sigma}^{\dagger} c_{i,\sigma}.$$

Here i in j run over the sites of the molecule, i.e., the p_z orbitals on each of the carbon atoms, $c_{i,\sigma}^{\dagger}$ and $c_{i,\sigma}$ are the electron creation and anihilation operator, respectively, for site i and spin σ , and $n_{i,\sigma} = c_{i,\sigma}^{\dagger} c_{i,\sigma}$ is the electron number operator. ε_i are the on-site energies controlled by the top gate voltage with energy zero being the Fermi-energy in the leads in the limit of zero source-drain bias. They may also be influenced by the electrodes attached to the leads. To be specific in what follows, we assign a uniform on-site energy ε_0 to all molecular sites, which includes the effect of the top gate voltage. However, we allow on-site energies on the two sites where the leads are attached to the molecule to take a different value of ε_1 . γ_{ji} are hopping integrals. Taking into account that next nearest neighbor hopping integrals in graphene are

at least an order of magnitude smaller than nearest neighbor hopping integrals²⁶, in what follows we neglect all but nearest neighbor hopping integrals, for which we take a uniform value of γ_1 .

The leads, modelled as carbon-atom chains with sites connected by nearest neighbor hopping integrals γ_0 , have Hamiltonian,

$$H_{\text{leads}} = \sum_{\alpha,i,\sigma} \varepsilon_{\alpha,i} n_{\alpha,i,\sigma} - \gamma_0 \sum_{\alpha,i,\sigma} c_{\alpha,i+1,\sigma}^{\dagger} c_{\alpha,i,\sigma} + \text{H.c.}$$

Here $\alpha \in \{s,d\}$ labels the source and drain leads, respectively, and i runs over the sites of a lead. $c_{\alpha,i,\sigma}^{\dagger}$, $c_{\alpha,i,\sigma}$ and $n_{\alpha,i,\sigma} = c_{\alpha,i,\sigma}^{\dagger} c_{\alpha,i,\sigma}$ are the electron creation, anihilation operator and the electron number operator for lead sites, respectively.

The couplings between leads and the molecule are

$$H_{\text{coupling}} = -V \sum_{\alpha,\sigma} c^{\dagger}_{\alpha,1,\sigma} c_{i_{\alpha},\sigma} + \text{H.c.}$$

Here V is the hopping integral between the lead site closest to the molecule and the molecular site i_{α} to which lead α is attached. The electron-electron and the electron-phonon interactions are not considered here the systems are not in the Coulomb blockade regime and the Kondo temperature is, due to weak Coulomb interaction regime considered here, much lower than temperatures of interest. However, some interesting features due to the electron correlations in benzene were found recently 27,28 . In the absence of many-body effects, the conductance of such a molecule, i.e., the propor-

In the absence of many-body effects, the conductance of such a molecule, i.e., the proportionality coefficient between the current through the molecule and the voltage $V_{\rm sd}$ applied between the source and the drain electrode, is, in the limit of vanishing $V_{\rm sd}$, given by the Landauer-Büttiker formula^{29,30},

$$G = G_0 \int \mathcal{T}(\varepsilon) \left(-\frac{\partial f(\varepsilon)}{\partial \varepsilon} \right) d\varepsilon,$$

where $G_0 = 2e^2/h$ is the conductance quantum, with e and h being the electron charge and the Planck constant, respectively. $\mathcal{T}(\varepsilon)$ is the transmission probability through the molecule at energy ε . $f(\varepsilon) = (\exp \frac{\varepsilon - \mu}{k_B T} + 1)^{-1}$ is the equillibrium Fermi function of the leads with μ and T being their chemical potential and temperature, respectively, and k_B being the Botzmann constant. For the sake of convenience we set the chemical potential to the middle of the 80 band in the leads and vanishing on-site energies in the leads, $\mu = \varepsilon_{\alpha,i} = 0$. 81

To calculate the transmission probability $\mathcal{T}(\varepsilon)$ we need to find the scattering eigenstate 82 $|\psi\rangle$ of the Hamiltonian for an electron with energy ε and spin σ , incoming from the source 83 electrode, 84

$$H|\psi\rangle = \varepsilon |\psi\rangle.$$

We expand such an eigenstate in the local basis states of the molecule $c_{j,\sigma}^{\dagger}|0\rangle$ and the leads $c_{\alpha,i,\sigma}^{\dagger}|0\rangle$

87

$$|\psi\rangle = \sum_{i} \psi_{i} c_{i,\sigma}^{\dagger} |0\rangle + \sum_{\alpha,i} \psi_{\alpha,i} c_{\alpha,i,\sigma}^{\dagger} |0\rangle.$$

The wavefunction in the source electrode is a linear combination of an incoming and a reflected plane wave, $\psi_{s,j} = e^{-ikj} + re^{ikj}$, while the wavefunction in the drain electrode 88 consists of a transmitted wave, $\psi_{d,j} = te^{ikj}$. The wavevector k can be calculated from the dispersion relation of the leads, $\varepsilon = -2\gamma_0 \cos k$. r and t are the reflection and the transmission amplitude, respectively. The transmission probability is $\mathcal{T}(\varepsilon) = |t|^2$. 91 Here we demonstrate the method of calculating the transmission probability $\mathcal{T}(\varepsilon)$ for 92 the case of the simplest possible molecule, namely a single site with the on-site energy of ε_0 coupled to two leads. The Schrödinger equation for such a system reads as a set of linear 94 equations for t, r and ψ_0 95

$$-\gamma_0 \left(e^{-2ik} + re^{2ik} \right) - V\psi_0 = \varepsilon \left(e^{-ik} + re^{ik} \right),$$

$$-V \left(e^{-ik} + re^{ik} \right) + \varepsilon_0 \psi_0 - V t e^{ik} = \varepsilon \psi_0,$$

$$-V \psi_0 - \gamma_0 t e^{2ik} = \varepsilon t e^{ik}.$$

By eliminating r and ψ_0 we find the transmission amplitude,

$$t = \frac{i\frac{2V^2}{\gamma_0}\sin k}{\varepsilon - \varepsilon_0 + \frac{2V^2}{\gamma_0}e^{ik}}.$$

A Breit-Wigner resonance of width $\Gamma_0 = \Gamma_s + \Gamma_d$, where $\Gamma_s = \Gamma_d = \frac{2V^2}{\gamma_0}$ are the partial width due to coupling to the source and the drain electrode, respectively, forms at energy ε_0 in the transmission probability in the wide band limit where $\gamma_0 \gg \varepsilon, \varepsilon_0, \Gamma_0$,

$$\mathcal{T}\left(\varepsilon\right) = \frac{\left(\frac{\Gamma_{0}}{2}\right)^{2}}{\left(\varepsilon - \varepsilon_{0}\right)^{2} + \left(\frac{\Gamma_{0}}{2}\right)^{2}}.$$

Generalization to more general molecules with arbitrary topology is straightforward. In the limit of weak coupling to the leads, $\Gamma = \frac{2V^2}{\gamma_0} \ll \gamma_1$, the transmission probability consists of similar resonances, positioned at eigenenergies of the molecule.

103 Results

As shown in Fig. 2(a-c), sites of graphene-like molecules we consider in this work form a 104 bipartite lattice, i.e. they break up into two sublattices in such a way that unprimed sites 105 $1, 2, 3 \dots$, forming one sublattice, are connected only to primed sites $1', 2', 3' \dots$, forming the 106 other sublattice. The Hamiltonian of such a system possesses particle-hole symmetry³¹. In 107 the molecules considered here, this symmetry is actually weakly broken due to next nearest 108 neighbour hopping integrals γ_2 . Since, as discussed in Sec. 2, $\gamma_2/\gamma_1 \ll 1$ for structures con-109 sidered in this work, we neglect such terms in what follows. Therefore, the conductance as a 110 function of the top gate voltage ε_0 is even with respect to the particle-hole symmetric point 111 $\varepsilon_0 = 0$, where the Fermi energy of the leads coincides with the center of the HOMO-LUMO gap. This is shown in Fig. 2 where the zero temperature and room temperature conduc-113 tances are plotted as a function of top gate voltage for benzene, naphthalene and anthracene 114 molecules for a particular choice of sites to which electrodes are attached. The zero temper-115

ature conductance curves consist of a set of resonances, each corresponding to a molecular 116 level being at the Fermi energy of the electrodes. The width of a resonance measures the 117 coupling of the molecular level to the electrodes. Note that some of the resonances are split 118 due to degeneracy of molecular orbitals. At room temperature, i.e., $T = 300 \,\mathrm{K} \sim 0.01 \gamma_1$, 119 with $\gamma_1 = 2.5 \,\mathrm{eV}$ as appropriate for graphene³², thermal broadening only slightly lowers the 120 peak heights, increases their widths and broadens minima. Within the HOMO-LUMO gap 121 the effect of finite temperature is negligible at room temperature. As we will concentrate on 122 the vicinity of the center of the HOMO-LUMO gap in the rest of this work, the calculations 123 will be done at zero temperature in what follows. 124

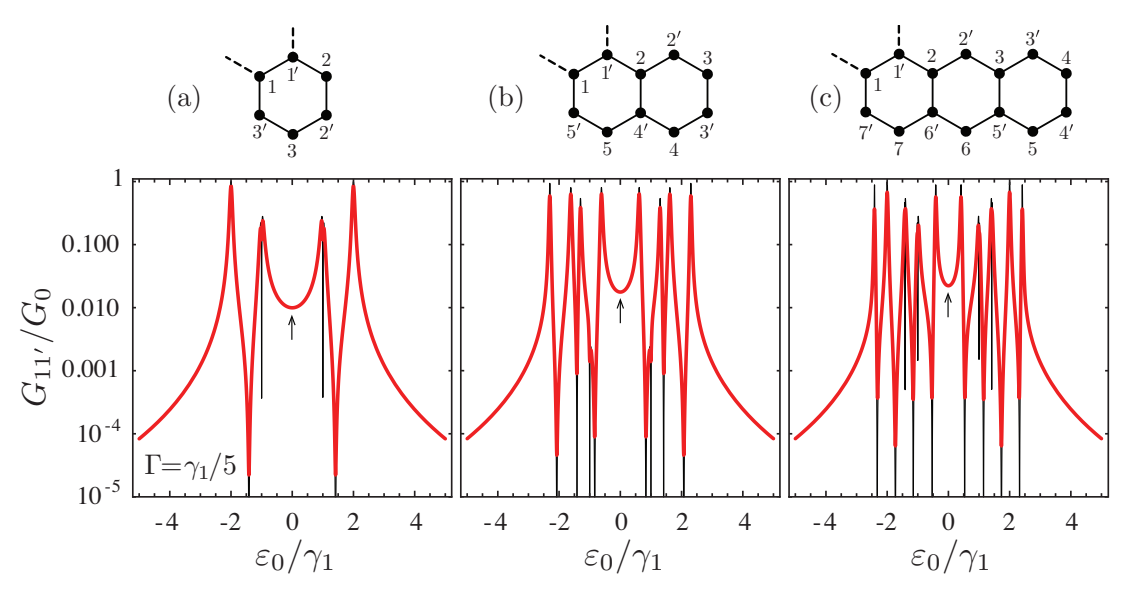


Figure 2: Conductance as a function of top gate voltage of the (a) benzene, (b) naphthalene, and (c) anthracene molecule when one electrode is connected to site 1 and the the other is connected to site 1' of the molecule, at T=0 (black lines) and at the room temperature (red lines). The coupling of an electrode to the molecular site is $\Gamma = \gamma_1/5$.

We now study the dependence of the conductance on the on-site energy ε_0 incorporating 125 the top gate voltage and the coupling Γ of an electode to a molecular site, for different 126 combinations of molecular sites to which the electrodes are attached. Let us first discuss the situation at the particle-hole symmetric point (indicated by arrows in Fig. 2), when the coupling to the leads Γ is weak²⁵. If the leads are connected to two sites in the same sublattice 129 the conductance is zero due to destructive interference. On the other hand, if the leads are 130

127

128

attached to two sites in distinct sublattices, a "magic integer" can be associated with such a 131 system. The ratio of conductances of two such systems is the so called "magic ratio" which 132 is a square of the ratio of the corresponding magic integers. In Fig. 3 we show how magic 133 ratios evolve with the coupling Γ increasing both at the particle hole symmetric point and 134 away from it at $\varepsilon_0 = \gamma_1/5$, which is still within the HOMO-LUMO gap of all the molecules 135 considered in this work. At the particle-hole symmetric point a magic ratio, provided its 136 weak coupling value is different from one, starts to deviate from its weak coupling value 137 when Γ becomes of the order of γ_1 . A magic ratio increases with Γ if its weak coupling value 138 is less than one and it decreases with Γ if its weak coupling value is larger than one. At 139 the particle-hole symmetry point $\varepsilon_0 = 0$ the deviation of magic ratios greater than one is 140 quadratic in Γ for $\Gamma \ll \gamma_1$. Away from the center of the HOMO-LUMO gap magic ratios 141 deviate from a square of the ratio of magic integers even in the weak coupling limit. The 142 deviation is again quadratic in ε_0 for $|\varepsilon_0| \ll \gamma_1$. At $\varepsilon_0 \neq 0$ a molecule conducts even if 143 electrodes are attached to sites in the same sublattice. Compared to the conductance when electrodes are attached to sites in different sublattices it is smaller by a factor of $(\varepsilon_0/\gamma_1)^2$ for 145 $|\varepsilon_0| \ll \gamma_1$. 146

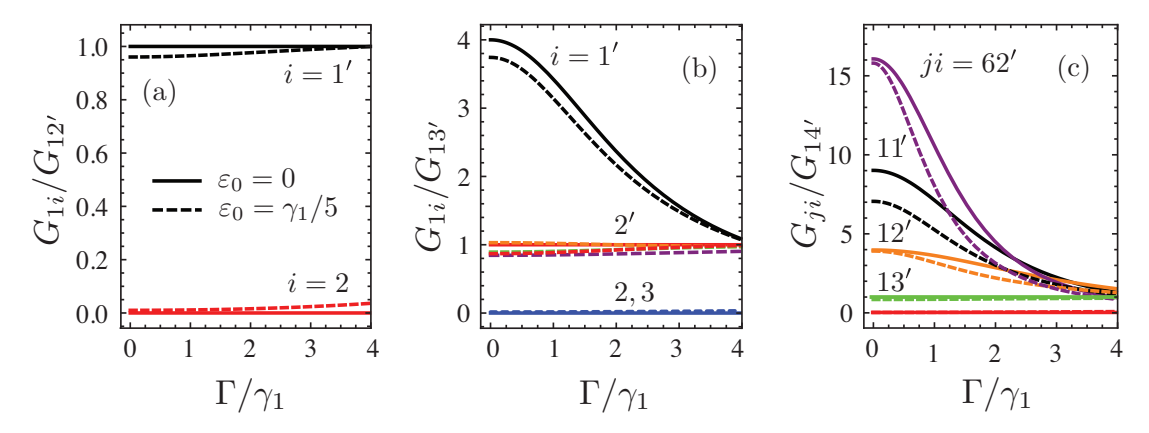


Figure 3: Magic ratios at T=0 of the (a) benzene, (b) naphthalene, and (c) anthracene molecule at the particle-hole symmetric point (full lines) and for $\varepsilon_0 = \gamma_1/5$ (dashed lines) as a function of the coupling Γ of an electrode to a molecular site. Molecular sites to which electrodes are attached are indicated next to each curve. The other combination of electrode attachment sites appearing in the conductance ratio corresponds to the most distant sites of a particular lattice.

An electrode may shift the on-site energy at the molecular site to which it is attached. This turns out to be another cause of deviation of a magic ratio from a square of the ratio of the magic integers. Fig. 4 displays that the departure of on-site energies ε_1 at these molecular sites from on-site energies $\varepsilon_0 = 0$ at other molecular sites causes a magic ratio to increase quadratically with ε_1 if it is larger than one for $\varepsilon_1 = 0$. A magic ratio is independent of ε_1 if it is equal to one for $\varepsilon_1 = 0$.

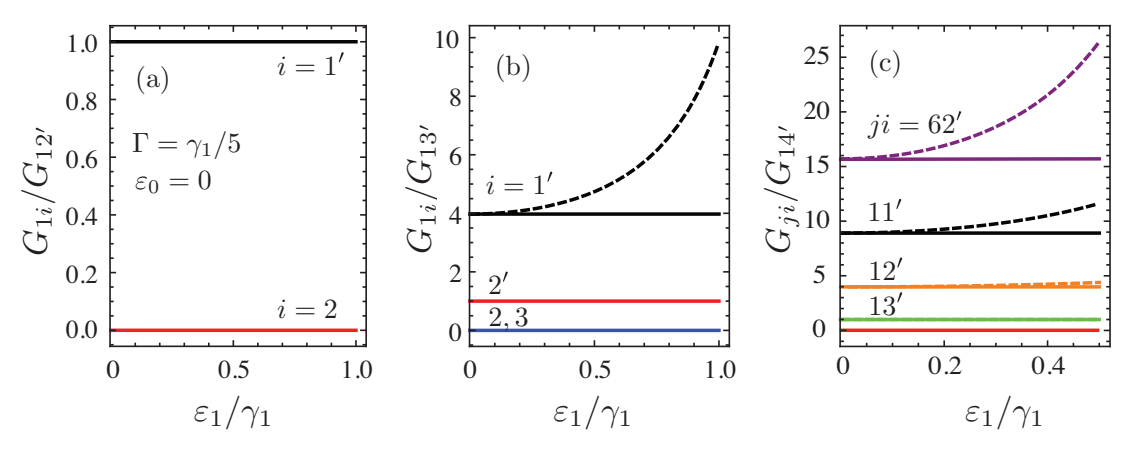


Figure 4: Magic ratios at T=0 of the (a) benzene, (b) naphthalene, and (c) anthracene molecule when the on-site energies ε_1 at molecular sites where the electrodes are attached differ from those at other molecular sites where $\varepsilon_0=0$ (dashed lines). Full lines show magic ratios for $\varepsilon_1=0$. Here $\Gamma=\gamma_1/5$.

153 Conclusions and outlook

In conclusion, we have calculated the ratios of conductances of graphene-like structures for 154 different combinations of sites to which electrodes are attached away from the regime where 155 those ratios can be expressed in terms of magic integers. The deviations were due to top 156 gate voltage pushing ε_0 away from the center of the HOMO-LUMO gap, due to the coupling 157 to electrodes Γ being non-negligible and due to the electrodes causing on-site energies ε_1 158 on atoms to which electrodes are attached to deviate from on-site energies on other atoms. 159 The deviation from the ratio given by magic integers was found to become important when 160 those parametes become of the order of the hopping integral γ_1 of the molecule. For small 161

values of those parameters, the deviation was found to increase proportionally to $(\varepsilon_0/\gamma_1)^2$, $(\Gamma/\gamma_1)^2$ or $(\varepsilon_1/\gamma_1)^2$. Furthermore, if the top gate voltage is non-zero, the molecule conducts even when both electrodes are attached to sites in the same sublattice, which for other perturbations is not the case. What remains to be done is to study the robustness of magic ratios to Coulomb interaction and to perturbations breaking the particle hole symmetry, i.e., the second neighbor hopping within the molecule.

168 Acknowledgement

The authors thank J. H. Jefferson for discussions and acknowledge support from the Slovenian Research Agency under contract No. P1-0044.

171 References

- (1) Datta, S. *Electronic Transport in Mesoscopic Systems*; Cambridge University Press:

 Cambridge, 1995.
- (2) Iniewski, K. Nano-Semiconductors: Devices and Technology; CRC Press taylor & Francis Group: Boca raton, 2012.
- (3) Likharev, K. K. IBM J. Res. Develop. **1989**, 32, 144.
- (4) Awschalom, D. D.; Bassett, L. C.; Dzurak, A. S.; Hu, E. L.; Petta, J. R. Science 2013,
 339, 1174.
- 179 (5) Chen, F.; Tao, N. Acc. Chem. Res. 2009, 42, 429.
- 180 (6) Pisula, W.; Feng, X.; Müllen, K. K. Chem. Mater. 2011, 23, 554.
- 181 (7) Kastner, M. A. Rev. Mod. Phys. **1992**, 64, 849.
- 182 (8) Hewson, A. C. *The Kondo Problem to Heavy Fermions*; Cambridge University Press:

 Cambridge, 1993.

- 184 (9) Rejec, T.; Ramšak, T.; Jefferson, J. H. J. Phys., Condens. Matter 2000, 12, L233–L239.
- 185 (10) Jefferson, J. H.; Ramšak, A.; Rejec, T. Europhys. Lett. **2006**, 74, 764.
- 186 (11) Mravlje, J.; Ramšak, A.; Rejec, T. Phys. Rev. B **2006**, 74, 205320.
- 187 (12) Mravlje, J.; Ramšak, A. Phys. Rev. B 2008, 78, 235416.
- 188 (13) Hong, W.; Valkenier, H.; Meszaros, G.; Manrique, D. Z.; Mishchenko, A.; Putz, A.;

 189 Garcia, P. M.; Lambert, C. J.; Hummelen, J. C.; Wandlowski, T.; Beilstein, J. Nan
 190 otechnology 2011, 2, 699.
- 191 (14) Vazquez, H.; Skouta, R.; Schneebeli, S.; Kamenetska, M.; Breslow, R.; Venkatara-192 man, L.; Hybertsen, M. *Nanotechnology* **2012**, *7*, 663.
- (15) Ballmann, S.; Hartle, R.; Coto, P. B.; Elbing, M.; Mayor, M.; Bryce, M. R.; Thoss, M.;
 Weber, H. B. Phys. Rev. Lett. 2012, 109, 056801.
- (16) Aradhya, S. V.; Meisner, J. A.; Krikorian, M.; Ahn, S.; Parameswaran, R.; Steigerwald, M. L.; Nuckolls, C.; Venkataraman, L. Nano Lett. 2012, 12, 1643.
- 197 (17) Kaliginedi, V.; Moreno-Garcia, P.; Valkenier, H.; Hong, W.; Garcia-Suarez, V. M.;
 198 Buiter, P.; Otten, J. L.; Hummelen, J. C.; Lambert, C. J.; Wandlowski, T. J. J. Am.
 199 Chem. Soc. 2012, 134, 5262.
- 200 (18) Aradhya, S. V.; Venkataraman, L. Nature Nanotechnology 2013, 8, 399.
- (19) Arroyo, C. R.; Tarkuc, S.; Frisenda, R.; Seldenthuis, J. S.; Woerde, C. H.; Eelkema, R.;
 Grozema, F. C.; van der Zant, H. S. Chemistry 2013, 125, 3234.
- (20) Guédon, C. M.; Valkenier, H.; Markussen, T.; Thygesen, K. S.; Hummelen, J. C.;
 van der Molen, S. J. Nature Nanotechnology 2012, 7, 305.
- ²⁰⁵ (21) Prins, F. Nano Letters **2011**, 11, 4607.

- (22) Cai, J.; Ruffieux, P.; Jaafar, R.; Bieri, M.; Braun, T.; Blankenburg, S.; Muoth, M.;
 Seitsonen, A. P.; Saleh, M.; Feng, X. Nature 2010, 466, 470.
- ²⁰⁸ (23) Ruffieux, P.; Cai, J.; Plumb, N. C.; Patthey, L.; Prezzi, D.; Ferretti, A.; Molinari, E.; Feng, X.; Mullen, K.; Pignedoli, C. A. *ACS Nano* **2012**, *6*, 6930.
- 210 (24) Cai, J.; Pignedoli, C. A.; Talirz, L.; Ruffieux, P.; Sode, H.; Liang, L.; Meunier, V.;

 Berger, R.; Li, R.; Feng, X. Nature Nanotechnology 2014, 9, 896.
- (25) Geng, Y.; Sangtarash, S.; Huang, C.; Sadeghi, H.; Fu, Y.; Hong, W.; Wandlowski, T.;
 Decurtins, S.; Lambert, C. J.; Liu, S.-X. Journal of the American Chemical Society
 2015, 137, 4469–4476.
- ²¹⁵ (26) Reich, S.; Maultzsch, J.; Thomsen, C.; Ordejón, P. Phys. Rev. B **2002**, 66, 035412.
- ²¹⁶ (27) Darau, D.; Begemann, G.; Donarini, A.; Grifoni, M. Phys. Rev. B **2009**, 79, 235404.
- ²¹⁷ (28) Valli, A.; Sangiovanni, G.; Toschi, A.; Held, K. Phys. Rev. B **2012**, 86, 115418.
- ²¹⁸ (29) Landauer, R. Philos. Mag. **1970**, 21, 863.
- 219 (30) Büttiker, M. Phys. Rev. Lett. 1986, 14, 1761.
- (31) Fazekas, P. Lecture Notes on Electron Correlation and Magnetism; Series in Modern
 Condensed Matter Physics; World Scientific: Singapure, 1999; Chapter 4, pp 147–197.
- (32) Castro Neto, A. H.; Guinea, F.; Peres, N. M. R.; Novoselov, K. S.; Geim, A. K. Rev.
 Mod. Phys. 2009, 81, 109–162.